# DEF6 deficiency, a mendelian susceptibility to EBV infection, lymphoma, and autoimmunity

Benjamin Fournier, Maud Tusseau, Marine Villard, Christophe Malcus, Emilie Chopin, Emmanuel Martin, Debora Jorge Cordeiro, Nicole Fabien, Mathieu Fusaro, Alexandra Gauthier, et al.

# Letter to the Editor

## DEF6 deficiency, a mendelian susceptibility to EBV infection, lymphoma, and autoimmunity

*To the Editor:*

DEF6/IBP/SLAT is a specific guanine nucleotide exchange factor for the Rho GTPase Cdc42 and Rac1. DEF6 is involved in T-cell receptor (TCR) signaling through its recruitment to the immune synapse.[1] *Def6*-deficient mice develop inflammation and autoimmunity symptoms and show variable immune defects, including abnormalities in $T_H$ cell differentiation, T-cell expansion, and germinal center formation.[2,3] Recently, Serwas et al[4] identified *DEF6* homozygous missense mutations in 3 patients from 2 families presenting with variable phenotypes, including recurrent infections and autoimmunity/autoinflammation signs with severe digestive and cardiac involvement. However, 2 of the 3 patients were also carrying a predicted pathogenic homozygous variant in *SKIV2L* (*SKIV2L*$^{Q1010fs*15}$), a gene whose deficiency leads to trichohepatoenteric syndrome (THES), which complicates understanding of the specific role of *DEF6* mutations in the patients' phenotype. Indeed, THES is characterized by intractable diarrhea, liver disease, developmental abnormalities, and combined immunodeficiency with T-cell and antibody defects.[5] The authors further showed that DEF6 deficiency impairs trafficking and expression of the checkpoint inhibitor CTLA4 in memory T regulatory (Treg) cells, which could contribute to autoimmunity in patients.[4]

Here, we have identified by whole exome sequencing a homozygous c.940C>T mutation in *DEF6* that led to a premature stop codon Q314* in 4 members of a consanguineous family with autoimmunity and susceptibility to EBV (Fig 1, *A* and *B*, Table I and see Fig E1 in this article's Online Repository at www.jacionline.org). Sanger sequencing confirmed the homozygous mutation in all 4 affected siblings of the family, whereas the parents were heterozygous (Fig 1, *A* and Table I). No other pathogenic variants were detected (see Fig E1, *B*). We failed to detect DEF6 expression in T-

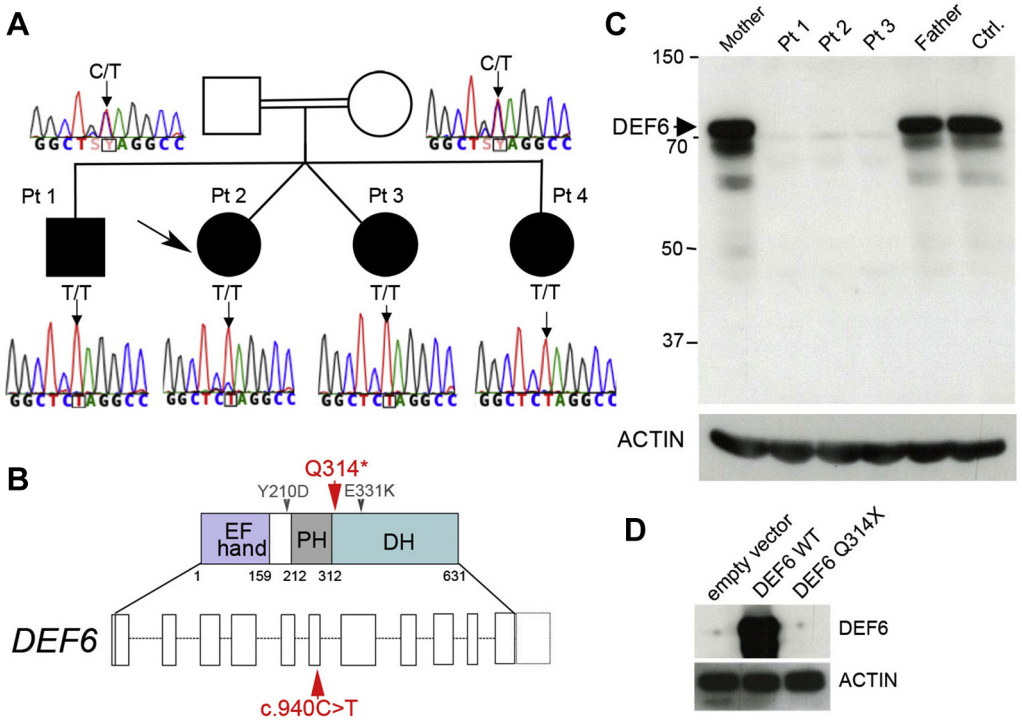


**FIG 1.** Identification of a homozygous nonsense mutation in *DEF6* in 4 siblings with autoimmunity, inflammation, chronic EBV viremia, and EBV-driven lymphoproliferations. **A**, Pedigree of the family with the proband indicated by an arrow. DNA electropherograms with an arrow showing the position of C in the wild-type allele, which is replaced by a T in the mutated allele. **B**, Diagram of *DEF6* intron-exon organization with the coding regions in white boxes, with their correspondence at the protein level with the different functional domains depicted, including the EF hand domain, the pleckstrin homology (PH) domain, and the Dbl homology (DH) domain. The mutation (c.940C>T, Q314*) is indicated by red arrows. Gray arrows indicate mutations previously reported by Serwas et al.[4] **C**, Western blot with anti-DEF6 antibody showing loss of DEF6 in cell lysates from T-cell blasts of the patients (Pt 1, Pt 2, Pt 3), mother, father, and 1 healthy control (Ctrl) (*upper panel*). Western blot with anti-ACTIN antibody as the loading control (*lower panel*). Size markers (in kDa) on the left. DEF6 is indicated by an arrow. **D**, Same as (**C**). Cell lysates of HEK 293 transiently transfected with an empty vector or a vector containing sequences for wild-type DEF6 (DEF6 WT) or mutated DEF6 (DEF6 Q314X). The residual band in lysates of the patients (**C**) and HEK 293 cells (**D**) with an empty vector or DEF6 Q314X likely corresponds to a nonspecific band.

**TABLE I.** Clinical phenotypes and immunologic parameters of patients with *DEF6* homozygous mutations

| Patient (Pt) | Pt 1 | Pt 2 | Pt 3 | Pt 4 | Pt 3** | Pt 1.1** | Pt 1.2** |
|---|---|---|---|---|---|---|---|
| Homozygous mutations | | | | | | | |
| DEF6 | p.Q31* | p.Q314* | p.Q314* | p.Q314* | p.Y210D | p.E331K | p.E331K |
| Other genes | | | | | | *SKIV2L* p.Q1010fs*15 | *SKIV2L* p.Q1010fs*15 |
| DEF6 protein expression | Strongly decreased | Strongly decreased | Strongly decreased | NA | Strongly decreased | Slight reduction | NA |
| Age at onset | 16 y | 10 y | 12 y | 17 mo | 7 mo | <1 mo | <1 mo |
| Ethnicity | Moroccan | Moroccan | Moroccan | Moroccan | Iraqi | Pakistani | Pakistani |
| Extrahematologic manifestations | Absent | Absent | Absent | Absent | Absent | IUGR Microcephaly Cardiac defect | IUGR Microcephaly Cardiac defect Liver failure |
| Recurrent and/or persistent infections | EBV | EBV | EBV | CMV‡ (PCR-positive, 1 episode) | CMV‡ (PCR-positive, 1 episode) | Bacterial sepsis Respiratory viruses | Bacterial sepsis |
| EBV virus load (log) | 4.5 | 5.2 | 5 | Neg | NM | NM | NM |
| EBV serology | IgG VCA$^+$ EBNA$^-$ | IgG VCA$^+$ EBNA$^-$ | IgG VCA$^+$ EBNA$^+$ | Neg | Neg at diagnosis | NM | NM |
| Immune manifestations | Rheumatoid purpura (1 episode) Cervical lymphadenopathy | EBV-positive Hodgkin lymphoma EBV-positive lymphoproliferations | Recurrent fever Tenosynovitis Arthritis | Severe AIHA | Severe AIHA | Severe watery diarrhea | Liver failure |
| Immuno phenotyping | | | | | | | |
| Inverted CD4$^+$/CD8$^+$ T-cell ratio | Yes | Yes | Yes | No | No | No | No |
| Diminution of naive CD4 T cells (CD31$^+$ CD45RA$^+$/CD4$^+$) | Yes | Yes | Yes | Yes | Yes (for CD3) | Yes (for CD3) | Yes (for CD3) |
| Excess of activated CD8$^+$ T cells (DR$^+$/CD8$^+$) | Yes | Yes | Yes | Yes | NM | NM | NM |
| Treg proportion (CD127$^{low}$CD25$^+$/CD4$^+$) | Normal | Slightly increased | Normal | Increased | Slightly reduced | Slightly reduced | NA |
| Memory Treg/unstimulated naive T conv | Decreased | Decreased | Decreased | Decreased | Decreased | Normal | NA |
| Excess >2% of FOXP3$^+$CD25CD4$^+$ T cells | Yes | Yes | Yes | NA | NM | NM | NM |
| Type 1 interferon signature | Neg | Positive | Positive | NA | NM | NM | NM |
| Autoantibodies | No | Anti-CaSR | ANCA | Direct Coombs test | Direct Coombs test | ANCA Cardiolipin $\beta_2$-GP | NA |
| Immunoglobulins (IgG, IgA, IgM) | Normal | Normal | Normal | Normal† | Normal | Decreased IgG | Normal |
| Vaccination responses (diphtheria, tetanus) | Variable | Normal | Normal | NA | NA | Decreased | NA |

*AIHA*, Autoimmune hemolytic anemia; *ANCA*, antineutrophil cytoplasmic antibodies; *IUGR*, intrauterine growth retardation ; *NA*, not assessed; *Neg*, negative; *NM*, not mentioned.
**Patients previously reported by Serwas et al.[4]
†Before immunosuppressive therapy.
‡Positive PCR result at onset of AIHA.

cell blasts from patients or when the DEF6$^{Q314*}$ mutant was transiently expressed in HEK 293 cells either without or with an N-terminal DYK-tagged protein (Fig 1, *C* and *D* and see Fig E1, *C*). These findings suggest that the Q314* mutation is a null mutation leading to a complete loss of DEF6 expression. At the age of 10 years, the index case patient (patient 2) experienced an EBV-positive nodular sclerosis classic Hodgkin lymphoma (HL) (see Fig E2 in this article's Online Repository at www.jacionline.org) treated by autologous stem cell transplantation, but the patient then presented with several episodes of lymphoproliferation associated with persistently high blood EBV loads (Table I and see Fig E2). As mouse Def6 is a negative regulator of follicular helper T cells ($T_{FH}$),[3] we characterized the T-cell infiltration in tumoral lymph nodes from patient 2. Staining for BCL6, a key transcriptional factor for $T_{FH}$ cells, displayed an infiltrate of $T_{FH}$ cells considered to be similar to that seen in other HLs (see Fig E2). In the first year of life, the youngest child (patient 4) developed (concomitantly to a transient, asymptomatic, and spontaneously resolutive cytomegalovirus [CMV] replication) a severe autoimmune hemolytic anemia and thrombocytopenia (hemoglobin level 3.5 g/dL with a highly positive Coombs test result) requiring repeated blood transfusions (see Fig E2). Treatment involving administration of corticosteroids, rituximab, azathioprine, and bortezomib as well as plasma exchanges had moderate efficacy (see Fig E2). The other 2 siblings had less severe clinical phenotypes. The eldest child (patient 1) is currently healthy, but he has a history of Henoch-Schönlein purpura and recently developed cervical lymph node enlargement with spontaneous regression. Since the age of 12 years, the other twin sister (patient 3) has had tenosynovitis with a slight increase of her C-reactive protein level (from 15 to 27 mg/mL) associated with recurrent fevers. Similarly to patient 2, patients 1 and 3 also showed abnormal detectable blood EBV loads (>4 log copies/mL) over 6 months (see Fig E2), whereas patient 4 has not yet encountered EBV (Table I). Except for CMV in patient 4, there was no evidence for other viral infection. The results of testing for autoantibodies were positive in 3 of 4 siblings (Table I). The twin sisters had a positive interferon signature in whole blood cells. Immunophenotyping showed slight abnormalities with an inverted $CD4^+$ to $CD8^+$ T-cell ratio associated with a decreased level of $CD45RA^+$ naive $CD4^+$ T cells and an excess of activated $HLADR^+CD8^+$ T cells (Table I and see Tables E1 and E2 in this article's Online Repository at www.jacionline.org). Additionally, we observed an increase of $FOXP3^+CD25^-CD4^+$ T cells in patients 1, 2, and 3, and in agreement with Serwas et al,[4] CTLA4 expression in memory Treg cells versus unstimulated naive conventional T (Tconv) cells (Treg/Tconv) was significantly reduced in both stimulated (CD3/CD28) and unstimulated memory Treg cells when compared to controls (Table I and see Table E1 and Fig E3 in this article's Online Repository at www.jacionline.org). Lymphocyte proliferation; activation-induced cell death; and $CD8^+$ T-cell degranulation following PHA, CD3, and CD3/CD28 stimulation and vaccination responses were normal or slightly diminished (Table I and see Table E1 and see Fig E4 in this article's Online Repository at www.jacionline.org). Immunoglobulin levels were normal, as were the levels of peripheral B-cell subsets. Despite the proposed role of mouse Def6 in TCR signaling,[1] analyses of TCR signaling in patients 1, 2, and 3 (including global tyrosine phosphorylation, phosphorylation of ZAP-70, PLC-γ1, ERK, NFAT2C degradation, and calcium flux) did not reveal any significant abnormalities (see Fig E4).

The 4 patients reported here did not have cardiac or digestive abnormalities and did not experience severe or opportunistic infections (except EBV). In Serwas et al,[4] all of these symptoms were restricted to both carriers of an additional *SKIV2L* variant (Table I). The third patient identified by Serwas et al[4] presented with a DEF6 deficiency alone, and he developed autoimmune anemia only in a context of CMV infection, which is a phenotype close to that of patient 4 reported here (Table I), suggesting a trigger role of CMV. Autoimmunity in patients with DEF6 deficiency may result from impaired Treg cell differentiation and function related to impaired CTLA4 recycling as found by Serwas et al.[4] We also observed expansion of unusual $FOXP3^+CD25^-$ Treg cells that may represent immature Treg cells or precursors (see Fig E3).[6] Interestingly, a similar population was previously reported in patients with systemic lupus erythematosus (SLE).[7] However, other abnormalities in T-cell differentiation, such as the increased $T_H17$ and $T_{FH}$ counts that have been documented in *def6*-deficient mice, may also participate to manifestations of autoimmunity and/or inflammation.[2] Apart from EBV, *DEF6* appears not to be critical to controlling other pathogens, similarly to genes that are restricted to the immune response to EBV, such as *ITK*, *CD70,* or *CD27*.[8] These genes are essential for the anti-EBV $CD8^+$ effector T-cell response. Interestingly, ITK-deficient patients present a strong predisposition to development of EBV-positive HL, and as DEF6 can be a direct substrate for ITK,[9] one might hypothesize that ITK deficiency is associated with impaired DEF6 function(s). Although we failed to detect gross abnormalities in proliferation and function of DEF6-deficient T cells, including CD27- and CD137/TNFRSF9/4-1BB–dependent T-cell proliferation (see Fig E5 in this article's Online Repository at www.jacionline.org), we assume that DEF6 is necessary for anti-EBV immunity. Additional experiments are warranted to determine the exact role of DEF6 in the immune control of EBV. In conclusion, we have provided evidence that DEF6 deficiency is a new inherited immune dysregulation disorder with variable expressivity ranging from autoimmunity and/or inflammation to EBV-associated lymphoproliferation and lymphoma without extrahematopoietic manifestations.

We thank the patients and the family for their participation in this study. We acknowledge Dr Boztug (Medical University of Vienna, Austria) for his gift of polyclonal anti-DEF6 antibody. We thank the Imagine Institute's Genomic and Bioinformatic platforms for their help in this work.

*Benjamin Fournier, MD*[a,b]*
*Maud Tusseau, MSc*[c]*
*Marine Villard, PhD*[d]
*Christophe Malcus, PharmD, PhD*[e]
*Emilie Chopin, MSc*[f]
*Emmanuel Martin, PhD*[a,b]
*Debora Jorge Cordeiro, PharmD*[a,b]
*Nicole Fabien, PharmD, PhD*[d]
*Mathieu Fusaro, PharmD*[a,g]
*Alexandra Gauthier, MD*[h]
*Nathalie Garnier, MD*[h]
*David Goncalves, PharmD*[d]
*Sonia Lounis, MSc*[a,b]
*Christelle Lenoir, MSc*[a,b]
*Anne-Laure Mathieu, PhD*[c]
*Marion Moreews, MSc*[c]
*Magali Perret, MSc*[d]
*Capucine Picard, MD, PhD*[a,b,g]
*Cécile Picard, MD*[i]

*Françoise Poitevin, PharmD*[e]
*Sébastien Viel, PharmD, PhD*[c,d]
*Yves Bertrand, MD, PhD*[c,h]
*Thierry Walzer, PhD*[c]
*Alexandre Belot, MD, PhD*[c,j,k]‡
*Sylvain Latour, PhD*[a,b]‡

From [a]the Laboratory of Lymphocyte Activation and Susceptibility to EBV infection, Institut National de la Santé et de la Recherche Médicale (Inserm) UMR 1163, F-75015, Paris, France; [b]Université de Paris, Imagine Institute, F-75015, Paris, France; [c]the International Center for Infectiology Research, Inserm U1111, Ecole Normale Supérieure de Lyon, Université Lyon 1, CNRS, UMR5308, Lyon, France; [d]the Immunology Department, Centre Hospitalier Lyon Sud, Pierre-Bénite, Lyon 1 University, France; [e]the Immunology Laboratory, Hôpital Edouard Herriot, Hospices Civils de Lyon, Lyon, France; [f]the Centre de Biotechnologie Cellulaire, Centre de Biologie et Pathologie Est, Hospices Civils de Lyon, Bron, France; [g]the Study Center for Primary Immunodeficiencies, Assistance Publique Hôpitaux de Paris, Necker-Enfants Malades Hospital, F-75015, Paris, France; [h]the Institut d'Hématologie et d'Oncologie Pédiatrique, Hospices Civils de Lyon, Lyon, France; [i]the Institut de Pathologie Multisite, Groupement Hospitalier Est, Hospices Civils de Lyon, UCBL Lyon 1 University, Lyon, France; [j]the National Referee Centre for Rheumatic and AutoImmune and Systemic diseases in childrEn (RAISE), France; [k]the Pediatric Nephrology, Rheumatology, Dermatology Unit, Hôpital Femme Mère Enfant, Hospices Civils de Lyon, University Lyon I, Lyon, France. E-mail: alexandre.belot@chu-lyon.fr. Or: sylvain.latour@inserm.fr.

*These authors contributed equally to this work.

‡These authors are co-last corresponding authors.

This study was funded by the Ligue Contre le Cancer-Equipe Labellisée (France) (to S.L.), INSERM (France), Rare Diseases Foundation (to S.L.) (France), ANR-14-CE14-0028-01 (to S.L.), ANR 18-CE15-0025-01 (to S.L.), "Investissements d'avenir" program ANR-10-IAHU-01 (Imagine Institute), the Société Française Société Française de Lutte contre les Cancers et Leucémies de l'Enfant et de l'Adolescent, AREMIG (France), Fédération Enfants et Santé (to S.L.) (France). B.F. is the recipient of a Fondation pour la Recherche Médicale fellowship (FDM20170638301) (France). D.J.C. was supported by the Imagine Institute PhD program funded by the Fondation Bettencourt Schueller. S.L. is a senior scientist at the Centre National de la Recherche Scientifique-CNRS (France).

Disclosure of potential conflict of interest: The authors declare that they have no relevant conflicts of interest.

## REFERENCES

1. Fos C, Becart S, Canonigo Balancio AJ, Boehning D, Altman A. Association of the EF-hand and PH domains of the guanine nucleotide exchange factor SLAT with $IP_3$ receptor 1 promotes $Ca^{2+}$ signaling in T cells. Sci Signal 2014;7:ra93.
2. Fanzo JC, Yang W, Jang SY, Gupta S, Chen Q, Siddiq A, et al. Loss of IRF-4-binding protein leads to the spontaneous development of systemic autoimmunity. J Clin Invest 2006;116:703-14.
3. Yi W, Gupta S, Ricker E, Manni M, Jessberger R, Chinenov Y, et al. The mTORC1-4E-BP-eIF4E axis controls de novo Bcl6 protein synthesis in T cells and systemic autoimmunity. Nat Commun 2017;8:254.
4. Serwas NK, Hoeger B, Ardy RC, Stulz SV, Sui Z, Memaran N, et al. Human DEF6 deficiency underlies an immunodeficiency syndrome with systemic autoimmunity and aberrant CTLA-4 homeostasis. Nat Commun 2019;10:3106.
5. Vély F, Barlogis V, Marinier E, Coste ME, Dubern B, Dugelay E, et al. Combined immunodeficiency in patients with trichohepatoenteric syndrome. Front Immunol 2018;9:1036.
6. Schuster M, Plaza-Sirvent C, Visekruna A, Huehn J, Schmitz I. Generation of Foxp3+CD25− regulatory T-cell precursors requires c-Rel and IκBNS. Front Immunol 2019;10:1583.
7. Horwitz DA. Identity of mysterious CD4+CD25-Foxp3+ cells in SLE. Arthritis Res Ther 2010;12:101.
8. Latour S, Tangye S. Primary immunodeficiencies reveal the molecular requirements for effective host defense against EBV infection. Blood 2020;135:644-55.
9. Hey F, Czyzewicz N, Jones P, Sablitzky F. DEF6, a novel substrate for the Tec kinase ITK, contains a glutamine-rich aggregation-prone region and forms cytoplasmic granules that co-localize with P-bodies. J Biol Chem 2012;287:31073-84.

https://doi.org/10.1016/j.jaci.2020.05.052

# METHODS

## Ethics

Written informed consent forms were obtained from all humans in this study in accordance with Declaration of Helsinki and local legislation and ethical guidelines from the Comité de Protection des Personnes de l'Ile de France II, Hôpital Necker-Enfants Malades, Paris. Blood from healthy donors was obtained at the Etablissement du Sang Français (Paris, France) under approved protocols (convention 15/EFS/012).

## Whole exome sequencing

Genomic DNA was extracted from whole blood according to the standard methods, and whole exome sequencing and data analysis were performed as previously described.[E1-E3] Genomic DNA regions flanking *DEF6* mutation were amplified by using the forward primer 5'-CTAAGGCCCCTTTCGGG C-3' and reverse primer 5'-GGCGCCGGGAGCTAACC-3' with Q5 High-Fidelity DNA Polymerase (NEB) according to the manufacturer's recommendations, gel-purified with a High Pure PCR Product Purification Kit (Roche), sequenced with a BigDye terminator v3.1 Cycle Sequencing Kit (Applied Biosystems, University Park, Ill), and analyzed on a 3500xL Genetic Analyzer (Applied Biosystems). All collected sequences were analyzed by using a DNADynamo (BlueTractorSoftware).

## Cell culture and stimulation

PBMCs were isolated by Ficoll-Paque (Lymphoprep, Proteogenix, France) density gradient centrifugation, washed, and resuspended at a density of $1 \times 10^6$ cells per mL in complete Panserin 401 medium (Pan Biotech, Germany) containing 5% human male AB serum (BioWest, France), 100 U/mL of penicillin, and 100 μg/mL of streptomycin (Gibco, Thermo Fischer Scientific, Waltham, Mass). T-cell blasts were expanded by incubating PBMCs for 72 hours with 2.5 μg/mL of PHA (Sigma-Aldrich, St Louis, Mo). Dead cells were then removed by Ficoll-Paque density-gradient (Lymphoprep, Proteogenix) centrifugation, and T-cell blasts were cultured in complete Panserin 401 medium culture supplemented with 100 IU/mL of recombinant human IL-2 (R&D Systems, Minneapolis, Minn). HEK293T cells were cultured in complete Dulbecco modified Eagle medium, high glucose, GlutaMAX supplement, pyruvate medium containing 10% heat-inactivated FCS (Gibco), 100 U/mL of penicillin, and 100 μg/mL of streptomycin (Gibco).

## Constructs

Wild-type *DEF6* coding sequence was obtained by RT-PCR from control T-cell blasts with the forward primer 5'-GACTAGTCCACCATGGCCCTGCGCAAG GAAC and the reverse primer 5'-ATAAGAATGCGGCCGCCTAATTTTCTG GTGCTGGATCC and inserted into the pCR 2.1-TOPO TA vector (Invitrogen, Carlsbad, Calif) according to manufacturer's instructions. The c.940C>T (p.Q314*) mutant was obtained with a Q5 Site-Directed Mutagenesis Kit (NEB, Ipswich, Mass) with the forward primer 5'-CGATCCGGCTCTAGGCCGAGGG and reverse primer 5'-CCATCTGGATGGCAGCTG. The N-terminal DYK-tagged wild-type and c.940C>T (p.Q314*) variants were obtained with a Q5 Site-Directed Mutagenesis Kit and the reverse primer 5'-ATCCTTGTAATCCATGGCTGAGGCG CCCGC. Coding sequences were confirmed by Sanger sequencing and subcloned into a bicistronic lentiviral vector encoding the mCherry protein as a reporter gene (pLVX-EF1alpha-IRES-mCherry Vector, ClonTech, Montain View, Calif).

## Transfections

HEK293T cells were transfected with empty pLVX-mCherry vector or pLVX-mCherry vector encoding wild-type and p.Q314* with lipofectamin 2000 (Invitrogen, Carlsbad, Calif) according to the supplier's instructions. Cells lysates were performed 48 hours after transfection.

## Immunoblotting

Cells were washed in PBS and lysed in lysis buffer (1% NP-40 [NP-40 alternative, Calbiochem], 50 mM Tris pH 8, 150 mM NaCl, 20 mM EDTA, 1 mM $Na_3VO_4$, 1 mM NaF, complete protease inhibitor cocktail (Roche), and phosphatase inhibitor cocktails 2 and 3 (Sigma). Cell lysates were clarified by centrifugation at 15,000 *g* for 5 minutes at 4°C. Supernatants were transferred to new tubes, and protein concentrations were determined by Coomassie protein assay reagent (Thermo Fischer Scientific). Next, 80 μg of proteins were denatured by boiling for 10 minutes with sample buffer (125 mM Tris pH 6.8, 3% SDS, 10% glycerol, 5% 2β-mercaptoethanol, and 0.01% bromophenol blue), separated by SDS-PAGE, and transferred on polyvinylidene difluoride membrane (Millipore, Burlington, Mass). Membranes were blocked with milk or BSA buffer before incubation with antibodies. The following antibodies were used for immunoblotting: anti-phosphorylated ERK1/2 (Phospho-p44/42 MAPK, 20G11, catalog no. 4376S), anti-phosphorylated PLCγ-1 (D6M9S, catalog no. 140008S), anti-phosphorylated tyrosine (P-Tyr-100, catalog no. 9411S), anti-phosphorylated ZAP-70 (catalog no. 2704S), anti-NFAT2 (D15F1, catalog no. 8032), and anti-DYKDDDDK Tag (D6W5B, catalog no. 14793S), all from Cell Signaling Technology (Danvers, Mass); anti–β-actin (A2066, Sigma-Aldrich; and anti-DEF6 (Abnova, catalog no. H000506 19-B01) (see Fig E1). The polyclonal anti-DEF6 antibody used in Fig 1 was a gift from Kaan Boztug (Medical University of Vienna, Austria) and was obtained from immunization with full-length DEF6 protein as previously described.[E4] Membranes were then washed and incubated with secondary anti-mouse (GE Healthcare, Chicago, Ill) or anti-rabbit (Cell Signalling Technology) horseradish peroxidase–linked antibodies. Pierce ECL Western blotting substrate was used for revelation. For reprobing, membranes were incubated with Restore Western Blot Stripping Buffer (Thermo Fischer Scientific) before blocking.

## Flow cytometry

Cell membrane staining and the flow cytometry–based phenotypic analyses were performed according to standard flow cytometry methods. The following validated antibodies were used: anti-CD45 (B3821F4), anti-CD3 (UCHT1), anti-CD4 (SFCI12T4D11, 13B8.2), anti-CD8 (SFCI21Thy2D3, B9.11), anti-CD19 (J3-119, HIB19), anti-CD20 (B9E9), anti-CD21 (BL13), anti-CD16 (3G8), anti-CD56 (N901, HCD56), anti-CD31 (5.6E), anti-CD197/CCR7 (G043H7), anti-CD45RA (2H4), anti-CD45RO (UCHL1), anti-CD14 (M5E2), anti-CD28 (CD28.2), anti-CD38 (HIT-2), anti-CD57 (NK.1), anti-CD62L (DREG-56), anti-CD107a/b (H4A3/HAB4), anti-CD161 (HP-3G10), and anti-TCR Vα7.2 (3C10), all purchased from Sony Biotechnology Inc; anti-CD16 (3G8), anti-IgD (IA6-2) from BD Biosciences; anti-TCRγδ (IMMY510), anti-TCR Vα24 (C15), and anti-TCR Vβ11 (X21) from Beckman Coulter (Fullerton, Calif); and anti-IgM (MHM88) from BioLegend. These antibodies were conjugated to fluorescein isothiocyanate (FITC), phycoerythrin (PE), PE–cyanine 5 (PE-Cy5), PE-Cy5.5, PE-Cy7, peridinin-chlorophyll (PerCP), PerCP-Cy5.5, allophycocyanin (APC), APC-Cy7, APC–violet 7 (APC-Vio7), Brilliant Violet 421 (BV421), Brilliant Violet 510 (BV510), Brilliant Violet 605 (BV605), Brilliant Violet 650 (BV650), Brilliant Violet 711 (BV711, or Brilliant Violet 785 (BV785). All data were collected on an LSRFortessa X-20 cytometer (BD Biosciences).

## Treg cell analysis by flow cytometry

Staining of fresh whole blood was performed as previously described[E5] by using PE-labeled anti-CD25 (B1.49.9), PE-Cy7–labeled anti-CD127 (R34.34), Alexa Fluor 647 (AF647)-labeled anti-FoxP3 (259D), and Pacific Blue–labeled antiCD4 (13B8.2) (Beckman Coulter). FOXP3-antibodies (clone 259D) were purchased from BioLegend (SanDiego, Calif). Briefly, cells were fixed and permeabilized by using the PerFix No-Centrifuge Assay Kit from Beckman Coulter according to the manufacturer's instructions. After permeabilization, cells were stained with fluorochrome-conjugated antibodies for 60 minutes and washed once with PBS and then with a solution containing formaldehyde. Cytometry analyses were performed on a NAVIOS flow cytometer using the NAVIOS software (Beckman Coulter).

## Proliferation assay

T-cell blasts were washed and cultured without IL-2 for 72 hours to synchronize the cells. T-cell blasts or PBMCs were labeled with Tag-it Violet

Proliferation and Cell Tracking Dye (Biolegend) according to the manufacturer's instructions. Cells were then cultured for 4 days in complete Panserin 401 medium alone or in the presence of 0.1, 1, or 10 μg/mL of immobilized anti-CD3 antibody (clone OKT3 [eBioscience]), and Dynabeads Human T-Activator CD3/CD28 (Invitrogen). Cells were surface-stained for CD3, CD4, CD8, and CD25 detection and analyzed by flow cytometry (LSRFortessa X-20 [BD Biosciences]). The proliferation index was calculated by using FlowJo software (TreeStar). Proliferation assays with cocultures of T cells with the P815 cells or lymphoblastoid cell line (LCL) cells have been previously described elsewhere.[E1,E6] Briefly, irradiated P815 expressing or not expressing CD137L or irradiated EBV B-cell lines (LCLs) expressing CD70 were preincubated with soluble 0.25 μg/mL anti-CD3 antibody, washed, and cocultured with PBMCs labeled with Cell Tracking Dye.

## Calcium flux analysis

$Ca^{2+}$ influx was assessed by real-time flow cytometry, as previously described.[E2] Briefly, cells were loaded with 5 μM Indo-1 AM (Molecular Probes, Eugene, Ore) in the presence of 2.5 mM probenecid (PowerLoad, Molecular Probes), washed, and surface-stained for CD4 and CD8 detection. Cells were analyzed in real-time with a FACS ARIA II flow cytometer (BD Biosciences). During acquisition, 1 μg/mL of anti-CD3 antibody was added to the cells, followed by 10 μg/mL of $F(ab')_2$ rabbit–anti-mouse IgG crosslinker (Jackson Immunoresearch), and finally incubated with a calcium ionophore (1 mM ionomycin [Sigma Aldrich]). Changes in the intracellular calcium concentration are quantified by a shift in the indo-1 emission peak from 485 nm (indo-blue) for unbound dye to 405 nm (indo-violet) when the indo-1 molecule is bound to calcium. Data were analyzed by using the kinetic tool of FlowJo software. Intracellular $Ca^{2+}$ levels correspond to the normalized ratio of 405-nm to 485-nm indo-1 emission peaks.

## Apoptosis assay

T-cell blasts were either left unstimulated or stimulated for 12 hours with 0.1, 1, and 10 μg/mL of immobilized anti-CD3 (clone OKT3).[E7] Briefly, cells were then washed and stained for viability (7-AAD viability staining [Biolegend]), for surface expression of CD3, CD4, and CD8 and surface localization of phosphatidylserines by FITC-conjugated Annexin-V (BD Bioscience). Cells were analyzed by flow cytometry; apoptotic cells corresponding to Annexin $V^+$/7-$AAD^-$ cells were quantified by using FlowJo software, and specific induced apoptosis was determined by using the formula: 100 × (% induced apoptosis – % spontaneous apoptosis)/(100 – % spontaneous apoptosis)).

## Degranulation assay

T-cell blasts were stimulated for 4 hours with 0.03, 0.3, 3, and 30 μg/mL of immobilized anti-CD3 in the presence of PE-conjugated anti-LAMP-1/2 (H4A3 and H4B4 [BD Biosciences]) as previously described.[E2] Cells were then washed and stained for surface expression of CD3 and CD8 and analyzed by flow cytometry.

## Immunochemistry

Biopsy specimens were fixed in 10% neutral buffered formalin, embedded in paraffin, and stained with hematoxylin and eosin. Immunohistochemical analyses were performed by routine protocols (Institut de Pathologie Multisite, Hospices Civils de Lyon) with the following commercially available antibodies: mouse mAb BCL6 (PG-B6p clone [Dako]), mouse mAb CD10 (56C6 clone [Novacastra]), mouse mAb PD1 (BioSB, Santa Barbara, Calif), mouse mAb CXCL3 (BCA-1 clone [R&D]), and mouse mAb ICOS (SP98 clone [Abcam]). The presence of EBV was demonstrated by *in situ* hybridization with a small RNA-encoding region 1 and 2 (EBER) probe (Ventana Medical Systems).

## CTLA4 staining

PBMCs were seeded to a 96-well flat-bottom plate at a density of $1.5 \times 10^6$ cells/mL and either left unstimulated or stimulated with anti-CD3/CD28 Dynabeads (Thermo Fisher) at a ratio of 0.8 bead for 1 cell. After 16 hours of incubation at 37°C, 95% humidity, and 5% $CO_2$, anti–CD4-FITC (RPA-T4 [BD]), anti–CD3-PerCP-Cy 5.5 (UCHT1 [BD]), anti-CD45RA-APC-Vio770 (T6D11 [Miltenyi Biotec]), and anti–CD7-BV510 (M-T701 [BD]) were added for surface staining for 30 minutes at 4°C. Cells were then fixed and permeabilized with the Foxp3 fixation/permeabilization staining buffer (eBioscience) and incubated with anti–CTLA4-PE (14D3 [eBioscience]) and anti–Foxp3-APC (PCH101 [eBioscience]) for 30 minutes at 4°C. Cells were acquired on a BD LSR Fortessa, and the data were analyzed by using FlowJo software. The ratio of CTLA4 expression of unstimulated or stimulated memory Treg cells to CTLA4 expression of unstimulated naive conventional Tconv cells was calculated as previously described.[E8]

## Interferon signature

Total RNA extraction was performed on whole blood collected on EDTA by using a Maxwell 16 LEV SimplyRNA Blood Kit (Promega, Madison, Wis) and a magnetic particle processor (Maxwell 16 [Promega]) according to the manufacturer's recommendations. The extraction kit included an individual DNAse treatment. Total RNA was diluted in 40 μL of RNAse-free water, and concentration was quantified by spectrophotometry by using a NanoVue (Biochrom). The first strand of cDNA was synthetized from 1 μg of total RNA by using a SuperScript VILO cDNA Synthesis Kit and Master Mix (Invitrogen). For the Nanostring (NanoString Technologies, Seattle, Wash) procedure, 200 ng of RNA was hybridized to the probes (a reporter probe and a capture probe) at 67 °C for 16 to 21 hours using a thermocycler. Samples were then inserted into the nCounter Prep Station for removal of excessive probes, purification, and immobilization onto the internal surface of a sample cartridge for 2 to 3 hours. Finally, the sample cartridge was transferred to the nCounter Digital Analyzer where color codes were counted and tabulated for each target molecule. Count numbers obtained for the 6 interferon-stimulated genes (ISGs) (ie, *IFIT1*, *SIGLEC1*, *IFI27*, *IFI44L*, *ISG15*, and *RSAD2*) were normalized by the geometric mean of the count numbers of 3 housekeeping genes (β-actin, hypoxanthine phosphoribosyltransferase 1 [HPRT1], and RNA polymerase II subunit A [POLR2A]) as well as the values of negative and positive controls by using nSolver software. The relative expression was determined for each normalized ISG expression by dividing by the median normalized expression of each ISG from a control group. Finally, the median of the relative expression of these 6 ISG was used to calculate the interferon score. The threshold was first defined as the mean of control group interferon score plus or minus 2 SD corresponding to a score of 2.3.

## REFERENCES

E1. Izawa K, Martin E, Soudais C, Bruneau J, Boutboul D, Rodriguez R, et al. Inherited CD70 deficiency in humans reveals a critical role for the CD70-CD27 pathway in immunity to Epstein-Barr virus infection. J Exper Med 2017;214:73-89.
E2. Demaret J, Saison J, Venet F, Malcus C, Poitevin-Later F, Lepape A, et al. Assessment of a novel flow cytometry technique of one-step intracellular staining: example of FOXP3 in clinical samples. Cytometry B Clin Cytom 2013;84:187-93.
E3. Martin E, Palmic N, Sanquer S, Lenoir C, Hauck F, Mongellaz C, et al. CTP synthase 1 deficiency in humans reveals its central role in lymphocyte proliferation. Nature 2014;510:288-92.
E4. Winter S, Martin E, Boutboul D, Lenoir C, Boudjemaa S, Petit A, et al. Loss of RASGRP1 in humans impairs T-cell expansion leading to Epstein-Barr virus susceptibility. EMBO Mol Med 2018;10:188-99.
E5. Demaret J, Saison J, Venet F, Malcus C, Poitevin-Later F, Lepape A, et al. Assessment of a novel flow cytometry technique of one-step intracellular staining: Example of FOXP3 in clinical samples. Cytometry B Clin Cytom 2013;84:187-93.
E6. Rodriguez R, Fournier B, Jorge Cordeiro D, Winter S, Izawa K, Martin E, et al. Concomitant *PIK3CD* and *TNFRSF9* deficiencies cause chronic active Epstein-Barr virus infection of T cells. J Exp Med 2019;216:2800-18.
E7. Rigaud S, Fondanèche M-C, Lambert N, Pasquier B, Mateo V, Soulas P, et al. XIAP deficiency in humans causes an X-linked lymphoproliferative syndrome. Nature 2006;444:110-4.
E8. Hou TZ, Verma N, Wanders J, Kennedy A, Soskic B, Janman D, et al. Identifying functional defects in patients with immune dysregulation due to LRBA and CTLA-4 mutations. Blood 2017;129:1458-68.

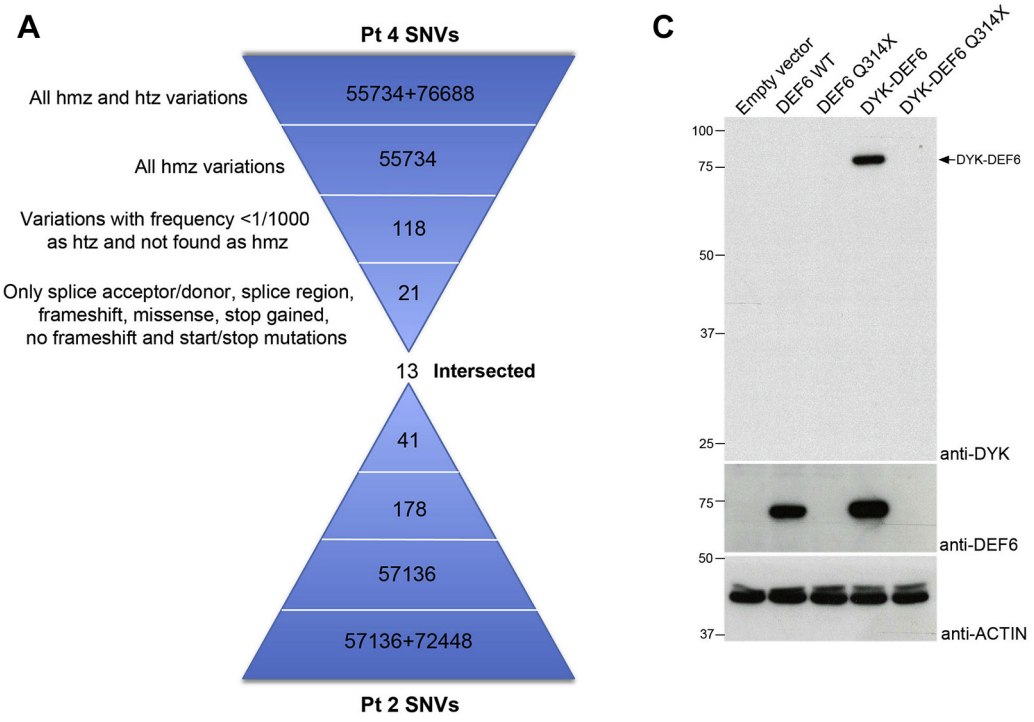


**B**

**Intersected variations of patients 2 and 4**

| Gene | Position GRCh37 | cDNA mutation | Amino Acid change | Type | CADD | gnomAD allele counts (htz/hmz/AF) |
|---|---|---|---|---|---|---|
| *DEF6* | 35285973 | c.C940T | p.Q314X | Stop-gained | 37 | NR |
| *UHRF1BP1* | 34826841 | c.T2708A | p.L903H | Missense | 27 | 3/0/1.21e-5 |
| *FBN3* | 8206715 | c.T751C | p. C251R | Missense | 26 | 11/0/4.38e-5 |
| *C19orf38* | 10970610 | c.G481C | p.A161P | Missense | 25 | 74/0/3.91e-4 |
| *ACOX2* | 58520731 | c.C103T | p.R35W | Missense | 24 | 188/1/6.65e-4 |
| *CLEC4G* | 7794902 | c.C627+4T | NA | Splice region | 14 | NR |
| *NFKBIZ* | 101572431 | c.C1061G | p.A354G | Missense | 11 | 15/0/5.3e-5 |
| *BRD4* | 15383618 | c.C285+8T | NA | Splice region | 8 | NR |
| *MUC22* | 30994106 | c.C898G | p.P300A | Missense | 1 | 5/0/1.73e-4 |
| | 30994110 | c.902_904delCCC | p.SP301S | Frameshift | NA | NR |
| | 30994117 | c.908_909insTGA | p.T303TE | Frameshift | NA | NR |
| | 30994124 | c.C916G | p.Q306E | Missense | 1 | NR |
| | 30994127 | c.A919G | p.T307A | Missense | 5 | NR |

AF, allele frequency. Htz, heterozygous. Hmz, homozygousNA, not applicable. NR, not reported

**FIG E1.** Identification of a *DEF6* nonsense homozygous mutation in patients 2 and 4. **A,** Analysis of the single-nucleotide variations (SNVs) detected by whole exome sequencing in the genome of patient (Pt) 2 and Pt 4. The numbers of SNVs are indicated in the triangles. SNVs were filtered by removal heterozygous (htz) variations present in public whole exome sequencing data bases and the data base of our institute with a frequency superior to 1/1000 found as homozygous (hmz), and finally removing nonfunctional intronic and synonymous mutations. **B**, The intersection (intersected) of the filtered SNVs in the 2 patients resulted in identification of 13 single common variations that were ordered given their combined annotation-dependent depletion (CADD) score, with *DEF6* variation having the highest correspondence to a nonsense/Stop gained mutation. **C,** Western blots with anti-DYK, anti-DEF6, and anti-ACTIN antibodies showing that *DEF6* Q314X is not detectable even when expressed with a tag (DYK). Cell lysates of HEK 293 transiently transfected with an empty vector or a vector containing sequences for wild-type DEF6 (DEF6 WT), mutated DEF6 (Q314X), or N-terminal DYK-tagged DEF6 forms (DYK-DEF6 and DYK-DEF6 Q314X). Cell lysates blotted with anti-ACTIN antibody as a loading control (*lower panel*). Size markers (in kDa) are on the left.

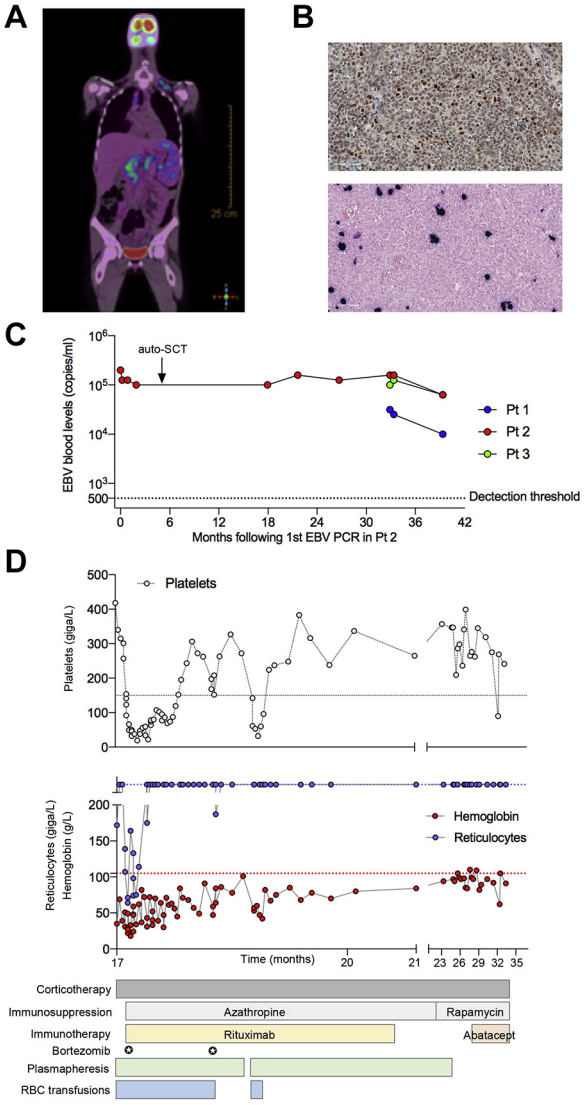


**FIG E2.** Clinical characterization and parameters of patients (Pt). **A,** Positron emission tomography imaging at the diagnosis of Hodgkin lymphoma in Pt 2. **B,** Immunostaining of the hepatic hilum lymph node surgical biopsy specimen showed positive heterogeneous BLC6 expression (*upper panel*), and *in situ* hybridization with an EBER probe stained multiple EBV-positive tumoral cells (*lower panel*) (magnification ×32). **C**, Evolution of blood EBV loads in Pts 1, 2, and 3. Autologous stem cell transplantation (auto-SCT) in Pt 2 is indicated by an arrow. **D,** Blood parameters and treatments of Pt 4 over a period of 17 months (age at the diagnosis of hemolytic anemia) to the age of 33 months. Upper panel shows platelet counts, with the horizontal dashed line corresponding to the lower normal limit of 150 billion platelets per liter. Middle panel shows hemoglobin and reticulocytes counts, with the horizontal red and blue dashed lines corresponding, respectively, to the lower normal limit of 110 g/L of hemoglobin and 200 billion reticulocytes per liter. Reticulocyte values higher than the threshold of 200 billion per liter are plotted on the blue line. Lower panels showed the different treatments implemented: abatacept, 10 to 20 mg/kg per injection; azathioprine, 2 mg/kg per day; bortezomib, 0.6 mg/kg per injection, with 4 injections per course; corticotherapy/corticosteroids, 0.4 to 4 mg/kg per day; rapamycin, 3 mg per day; and rituximab, 375 mg/m$^2$ per injection after each plasmapheresis course until complete B-cell depletion and then every 3 weeks. *RBC*, Red blood cell.

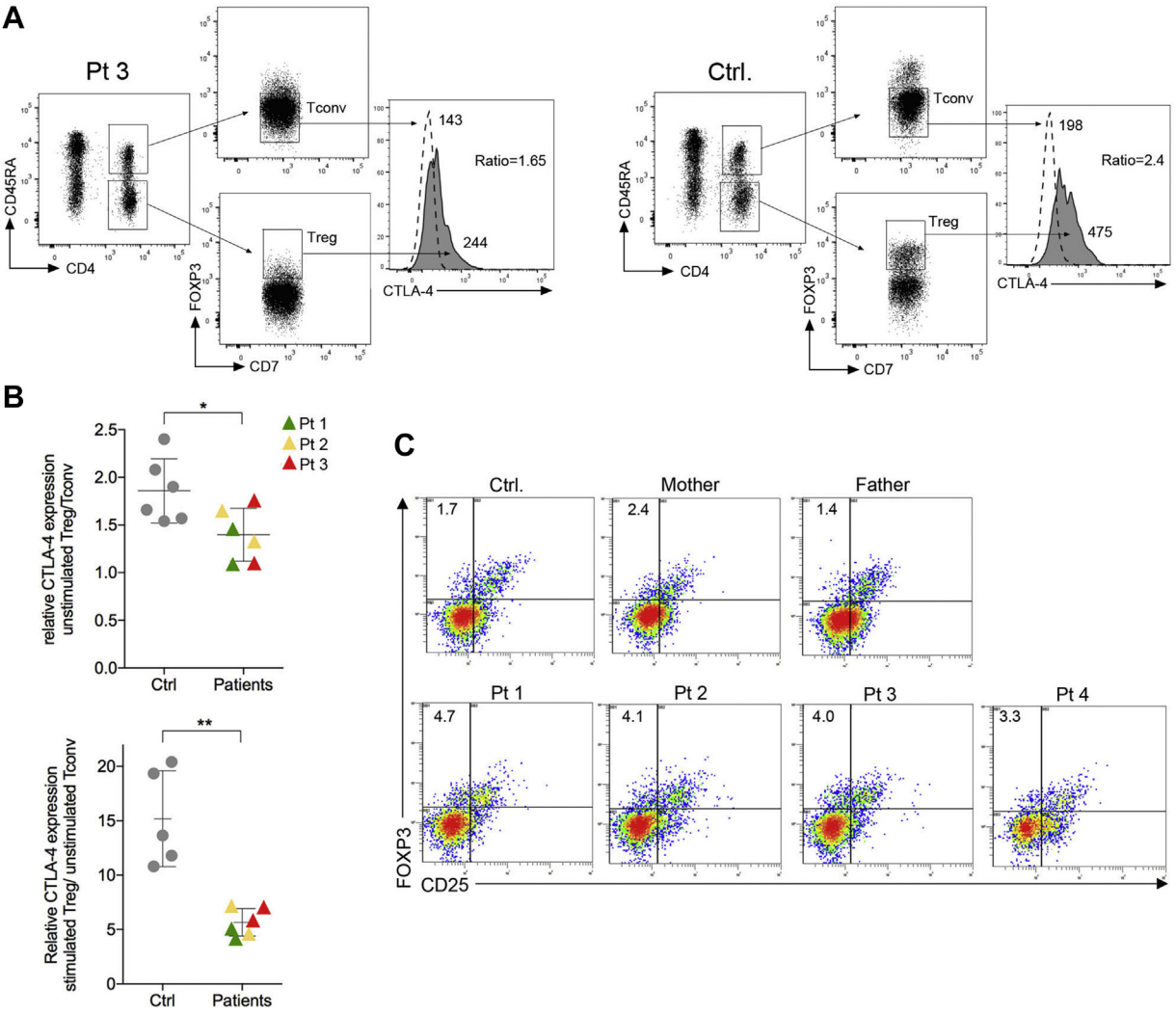


**FIG E3.** Characterization of Treg cells from patients 1, 2, 3, and 4 (Pt 1, Pt 2, Pt 3, Pt 4). **A** and **B,** Comparison of CTLA4 expression on unstimulated and stimulated Treg cells versus conventional T (Tconv) cells of controls (Ctrls) and Pts. **A,** Examples of fluorescence-activated cell sorting (FACS) analysis of CTLA4 expression on unstimulated Treg cells versus on Tconv cells of a control (Ctrl) and a Pt (Pt 3). Treg cells and Tconv cells were isolated by gating and correspond to $CD4^+CD45RA^-FOXP3^+$ and $CD4^+CD45RA^+FOXP3^-$ cells, respectively. The mean fluorescence intensities of CTLA4 expression on Treg cells and Tconv cells were calculated from histograms (*right panels*). The ratio of the CTLA4 mean fluorescence intensity of Treg cells to that of Tconv cells is indicated in the histogram plots of the control and the Pt. **B,** Graphs showing the comparison of CTLA4 expression on unstimulated (*upper panel*) or stimulated (*lower panel*) Treg cells and Tconv cells unstimulated from the Ctrl and from Pts 1, 2, and 3. Ratio calculated from FACS data as shown in (**A**) from 2 independent experiments. $*P < .05$; $**P < .01$ (Mann-Whitney *U* test). **C,** Phenotyping of Treg cells after gating on $CD4^+$ lymphocytes. Dot plots from FOXP3 and CD25 expression analyzed by FACS. The percentage of FOXP3+$CD25^-$ T cells is indicated on the upper left part of each dot plot. One experiment on 2 independent for Pt 1, Pt 2, and Pt 3 with similar results (5.1%, 3.3%, and 3.2% of $FOXP3^+CD25^-$, respectively).

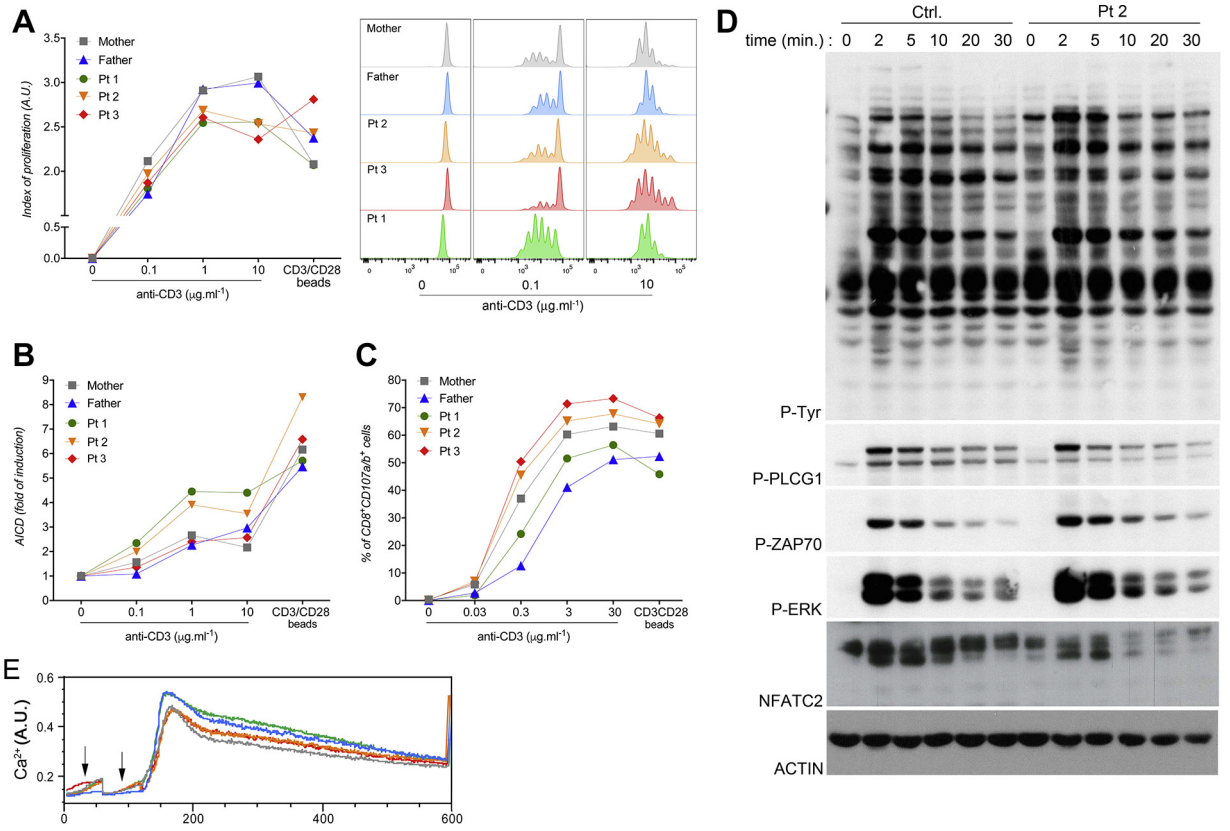


**FIG E4.** Functional characterization of T cells from patients (Pt) 1, 2, and 3 (Pt 1, Pt 2, and Pt 3). **A-C,** Analyses of T-cell blasts from DEF6-deficient Ps 1, 2, and 3 and their parents (Mother and Father). **A,** Cell proliferation profiles determined by dilution of CellTrace Violet (CTV) in response to immobilized anti-CD3 antibody at the indicated concentrations or anti-CD3/CD28–coated beads. Left panel shows index values in arbitrary units (A.U.) of proliferation calculated from CTV profiles shown as examples in the right panels for the stimulation with 0, 0.1, and 10 µg/mL of anti-CD3. **B,** Activation-induced cell death (AICD) after stimulation with the indicated concentration of anti-CD3. Apoptotic cells detected by annexin V (AV) and 7-AAD staining. Ratio of the percentage of apoptotic cells ($AV^+$/7-$AAD^-$ cells in the $CD3^+$ gates) in each condition to the percentage of unstimulated cells. **C,** Degranulation of $CD8^+$ T cells stimulated with the indicated concentrations of anti-CD3. Cells stained with antibodies against CD107a/b (LAMP1/2), a surface-exposed marker of the secretion of lytic granules. The percentages of $CD8^+CD107a/b^+$ are shown. **D,** Analysis of TCR signaling in T-cell blasts from a control donor (Ctrl) and a DEF6-deficient Pt (Pt 2). Immunoblots showing the phosphorylation of proximal signaling molecules after stimulation with anti-CD3 antibodies for 0, 2, 5, 10, 20, 30, and 60 minutes. Cell lysates immunoblotted with antibodies against tyrosine phosphorylated residues (P-Tyr), phosphoPLCG1 (P-PLCG1), phospho-ERK1/2 (P-ERK), NFAT2C, and phospho-ZAP-70 (P-ZAP70) and ACTIN as a loading control. The same data were obtained for Pt 1 and Pt 3. **E,** Flow cytometry analyses of $Ca^{2+}$ flux in T cells loaded with the $Ca^{2+}$-sensitive fluorescent dye Indo1. Cells then stimulated with anti-CD3 (*first arrow*) crosslinked with rabbit anti-mouse (*second arrow*). Intracellular $Ca^{2+}$ levels expressed in A.U. The colors are the same as in (**A-C**) corresponding to Pts and parents. **A-E,** Data from 1 experiment.

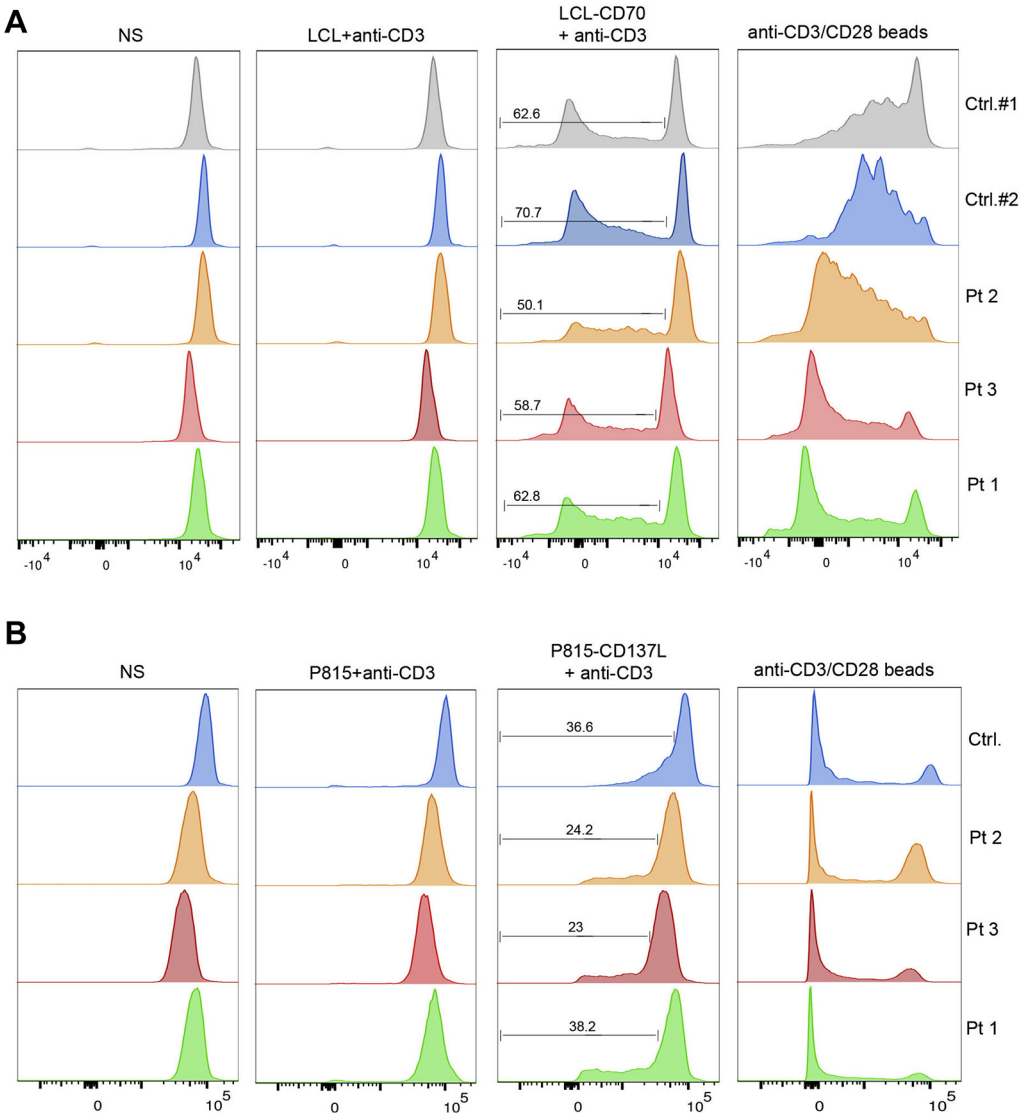


**FIG E5.** CD70-CD27– and CD137L-CD137–dependent T-cell proliferation of T cells of patients (Pt) 1, 2, and 3 (Pt 1, Pt 2, and Pt 3). Proliferation of T cells from PBMCs of controls (Ctrls) and Pts (Pts 1, 2, and 3) cocultured in **(A)** with irradiated LCL cells expressing or not CD70 (LCL-CD70) and in **(B)** with irradiated P815 cells expressing or not expressing CD137L (P815-CD137L). Irradiated LCL and P815 cells were preincubated with anti-CD3 antibody (+ anti-CD3) before being added to the PBMCs. Nonstimulated (NS) PBMCs were cultured without irradiated LCL or P815 cells. PBMCs were also cocultured with coated beads with anti-CD3/CD28 (anti-CD3/CD28–coated beads) as positive controls. Histograms of CellTrace violet dilution gated on $CD3^+$ cells. Percentages of proliferating T cells are indicated in the histogram plots for LCLs-CD70 and P815-CD137L.

**TABLE E1.** Immunologic parameters of the patients

| | Pt 1 | Pt 2 | Pt 3 | Pt 4* | Pt 4† | Pt 4‡ |
|---|---|---|---|---|---|---|
| **Patient parameter** | **Age 19 y** | **14 y** | **14 y** | **17 mo** | **18 mo** | **26 mo** |
| Leukocytes (cells/mm$^3$) | 7940 | 4380 | **4070** | 12787 | 6013 | **2450** |
| Neutrophils (cells/mm$^3$) | 5690 | 2370 | 2170 | — | — | **1320** |
| Monocytes (cells/mm$^3$) | 670 | 520 | 330 | — | — | 250 |
| Lymphocytes (cells/mm$^3$) | 1568 | 2210 | 1986 | **2623** | **657** | **763** |
| T cells | | | | | | |
| CD3$^+$ (cells/mm$^3$) | 1052 | 1615 | 1533 | **1240** | **611** | **557** |
| CD4$^+$ (cells/mm$^3$) | **395** | **495** | **615** | **668** | **173** | **181** |
| CD8$^+$ (cells/mm$^3$) | 537 | 968 | 751 | 517 | **394** | **315** |
| CD4/CD8 ratio | *0.73* | **0.51** | *0.82* | 1.29 | **0.44** | *0.58* |
| TCRγ/δ (%) | 11.9 | 12.2 | 9.4 | — | — | — |
| CD31$^+$CD45RA$^+$/CD4$^+$ (recent naive thymic emigrant) (%) | **22** | **40** | **30** | **39** | **—** | **16** |
| CD45RO$^+$/CD4$^+$ (memory) (%) | *70* | *58* | *59* | — | **—** | *68* |
| CCR7$^+$CD45RA$^+$/CD8$^+$ (naive) (%) | **16.4** | **16.4** | **31.5** | — | — | **2.3** |
| CCR7$^+$CD45RA$^-$/CD8$^+$ (central memory) (%) | **1.3** | **2.8** | **2.0** | — | — | 1.0 |
| CCR7$^-$CD27$^-$CD45RA$^-$/CD8$^+$ (effector memory) (%) | *61.5* | *59.5* | *36.4* | — | — | *35.8* |
| CCR7$^+$CD27$^-$CD45RA$^+$/CD8$^+$exhausted effector memory) (%) | *20.8* | *21.3* | *30.2* | — | — | *61.0* |
| CD127$^{low}$ CD25$^+$/CD4$^+$ (regulatory) (%) | 8.1 | *7.7* | 7 | — | — | *9.3* |
| Vα7$^+$CD161$^+$/CD3$^+$ (MAIT) (%) | 3.22 | **0.36** | **0.2** | — | — | — |
| Vα24$^+$Vβ11$^+$CD161$^+$/CD3$^+$ (iNKT) (%) | 0.17 | 0.11 | 0.043 | — | — | — |
| CD3$^+$DR$^+$ (%) | *27.9* | *38.8* | *25.7* | — | — | 31.1 |
| CD4$^+$DR$^+$ (%) | *9.1* | *11.1* | 7.2 | — | — | 17.9 |
| CD8$^+$DR$^+$ (%) | *40.2* | *55.2* | *39.9* | — | — | 39.9 |
| PHA *(%* CD3$^+$Edu$^+$*)* | 16 (mod.) | 7.8 (weak) | 13 (mod.) | — | — | — |
| OKT3 (50 ng/mL) *(%* CD3$^+$Edu$^+$*)* | 17 (good) | 8.9 (mod.) | 12.7 (good) | — | — | — |
| PWM *(%* CD3$^+$Edu$^+$*)* | 2.8 (good) | 2.0 (mod.) | 2.2 (good) | — | — | — |
| *Candida* (25 mg/L to 10 mg/L) *(%* CD3$^+$Edu$^+$*)* | 4.9 – 4.1 (mod.) | 5.6 – 0.9 (good) | 4.3 – 0.9 (mod.) | — | — | — |
| Tetanus toxoid (10 mg/L to 5 mg/L) *(%* CD3$^+$Edu$^+$*)* | 1.9—1.3 (weak) | 0.8 – 0.7 (weak) | 0.9 – 5.5 (mod.) | — | — | — |
| Tuberculin (10 mg/L to 5 mg/L) *(%* CD3$^+$Edu$^+$*)* | 8.9 – 5.8 (good) | 1.1 – 3.3 (mod.) | 8.1 – 8.8 (good) | — | — | — |
| NK cells | | | | | | |
| CD16$^+$CD56$^+$(cells/mm$^3$) | 366 | 219 | 171 | 340 | **21** | 159 |
| CD16$^+$CD56$^+$ (%) | 23 | 10 | 9 | 13 | 3 | *21* |
| B cells | | | | | | |
| CD19$^+$ (cells/mm$^3$) | 144 | **191** | **110** | 963 | — | **9** |
| CD19$^+$ (%) | 9.2 | 12 | **7** | 36.7 | **<0.5** | **1.2** |
| CD27$^+$/CD19$^+$ (memory) (%) | 18 | 14 | 15 | — | — | *78.1* |
| CD27-IgD$^+$/CD19$^+$ (naive) (%) | 71 | 80 | 82 | — | — | **17.7** |
| CD27$^+$IgD$^+$/CD19$^+$ (marginal zone-like B cells) (%) | 9 | 7 | 11 | — | — | *74.4* |
| CD27$^+$IgD$^-$/CD19$^+$ (switched memory) (%) | 9 | 7 | 4 | — | — | *4.3* |
| CD24$^{++}$CD38$^{++}$/CD19$^+$ (%) | 8 | 11 | 13 | — | — | — |
| CD24$^{++}$CD38$^{++}$CD27$^-$IgD$^+$/CD19$^+$ (transitional B cells) (%) | *8* | 11 | 13 | — | — | *15.4* |
| CD24$^-$CD38$^{++}$/CD19$^+$ (plasmablasts) (%) | 1 | 3 | 1 | — | — | — |
| CD21$^{low}$CD38$^{low}$/CD19$^+$ (%) | 5 | 5 | 5 | — | — | — |
| CD21$^{++}$CD24$^+$/CD19$^+$ (%) | 64 | 67 | 65 | — | — | — |
| IgG (g/L) | *15.6* | 12.3 | 12.3 | 11.7 | — | — |
| IgM (g/L) | 2.13 | 2.21 | 1.72 | 0.24 | — | — |
| IgA (g/L) | 0.83 | 1.10 | 1.34 | 0.73 | — | — |

*MAIT*, Mucosal invariant T cells; *PWN*, pokeweed mitogen.

Italics indicate values higher than the normal values; boldface indicates values less than the normal values (see Table E2); For lymphocyte proliferation, data are from routine tests. A weak proliferation corresponds to 0.5% to 15% or 0.5% to 2.5% of CD3$^+$EdU$^+$ cells after 72 hours or 7 days of stimulation with PHA or tetanus toxoid, respectively. A moderate *(mod.)* proliferation corresponds to 15% to 35%, 10% to 25%, 3% to 5%, or 2.5% to 5% of CD3$^+$EdU$^+$ cells after 72 hours of stimulation with PHA, OKT3, or PWN or 7 days with antigens, respectively. A good proliferation corresponds to more than 35%, more than 25%, more than 5%, or 5% to 15% of CD3$^+$EdU$^+$ cells after 72 hours of stimulation with PHA, OKT3, or PWN or 7 days with antigens, respectively.

*At the time of the phenotyping, the patient was receiving only corticosteroids.

†The patient was receiving rituximab injections in addition to corticosteroids and azathioprine.

‡The patient was treated with corticosteroids, rapamycin. and abatacept.

**TABLE E2.** Immunologic normal age-matched values for Table E1

| Age-matched normal value | At age 18 y | At age 10-15 y | At age 1-2 y |
|---|---|---|---|
| Leukocytes (cells/mm$^3$) | 4,100-10,500 | 4,100-10,500 | 6,000-17,500 |
| Neutrophils (cells/mm$^3$) | 1,800-6,300 | 1,500-6,400 | 1,500-8,500 |
| Monocytes (cells/mm$^3$) | 300-1,000 | 300-1,000 | 180-600 |
| Lymphocytes (cells/mm$^3$) | 1,000-3,400 | 1,500-4,000 | 4,000-10,500 |
| T cells | | | |
| $CD3^+$ (cells/mm$^3$) | 1,000-2,200 | 1,200-2,600 | 1,900-5,900 |
| $CD4^+$ (cells/mm$^3$) | 530-1,300 | 650-1,500 | 1,400-4,300 |
| $CD8^+$ (cells/mm$^3$) | 330-920 | 370-1,100 | 500-1,700 |
| CD4/CD8 ratio | 0.6 | 0.6 | 0.6 |
| $CD31^+CD45RA^+/CD4^+$ (recent naive thymic emigrant) (%) | 51-79 | 50-78 | 48-76 |
| $CD45RO^+/CD4^+$ (memory) (%) | 27-50 | 28-49 | 4.5-17.5 |
| $CCR7^+CD45RA^+/CD8^+$ (naive) (%) | 48-87 | 62-86 | 77-98 |
| $CCR7^+CD45RA^-/CD8^+$ (central memory) (%) | 10-37 | 12-27 | 1-8 |
| $CCR7^-CD27^-CD45RA^-/CD8^+$ (effector memory) (%) | 0.2-7 | 1-6 | 0-2.8 |
| $CCR7^+CD27^-CD45RA^+/CD8^+$ (exhausted effector memory) (%) | 0.8-14 | 0.8-13 | 0-11 |
| $CD127^{low}CD25^+/CD4^+$ (regulatory) (%) | 4.0-10.0 | 2.8-7.2 | 2.9-7.4 |
| $V\alpha7^+CD161^+/CD3^+$ (MAIT) (%) | 1-8 | 1-8 | 1-8 |
| $V\alpha24^+V\beta11^+CD161^+/CD3^+$ (iNKT) (%) | >0.02 | >0.02 | >0.02 |
| $CD3^+$ $DR^+$ (%) | 1.3-12.2 | 5.0-12.5 | 4.5-14.5 |
| $CD4^+$ $DR^+$ (%) | 0.7-4.6 | 4.0-11.0 | 3.0-12.0 |
| $CD8^+$ $DR^+$ (%) | 0.3-4 | 5.0-25.0 | 7.0-37.0 |
| Natural killer cells | | | |
| $CD16^+CD56^+$ (cells/mm$^3$) | 70-480 | 100-480 | 160-950 |
| $CD16^+CD56^+$ (%) | 3-22 | 4-17 | 3-15 |
| B cells | | | |
| $CD19^+$ (cells/mm$^3$) | 110-570 | 270-860 | 610-2,600 |
| $CD19^+$ (%) | 6-23 | 13-27 | 14-37 |
| $CD27^+/CD19^+$ (memory) (%) | 7-29 | 9-35 | 3.5-12.2 |
| $CD27^-IgD^+/CD19^+$ (naive) (%) | 65.6-79.6 | 61.6-87.4 | 69.2-90.5 |
| $CD27^+IgD^+/CD19^+$ (marginal zone–like B cells) (%) | 7.4-13.9 | 2.6-13.4 | 4.6-16.3 |
| $CD27^+IgD^-/CD19^+$ (switched memory) (%) | 7.2-12.7 | 4-21.2 | 0-4 |
| $CD24^{++}CD38^{++}CD27^-IgD^+/CD19^+$ (transitional B cells) (%) | 1-5.7 | 1.4-13 | 3.0-13.1 |
| $CD24^-CD38^{++}/CD19^+$ (plasmablasts) (%) | 0.4-2.4 | 0.6-6.5 | |
| $CD21^{low}CD38^{low}/CD19^+$ (%) | 1.6-10 | 2.7-8.7 | |
| IgG (g/L) | 6.4-13 | 6.4-13 | 3-15 |
| IgM (g/L) | 0.56-3.52 | 0.56-3.52 | 0.25-1.15 |
| IgA (g/L) | 0.7-3.12 | 0.7-3.12 | 0.16-1 |

*iNKT*, Invariant natural killer cells; *MAIT*, mucosal invariant T cells.